

NOSC TR 1143

12

NOSC TR 1143

DTIC FILE COPY

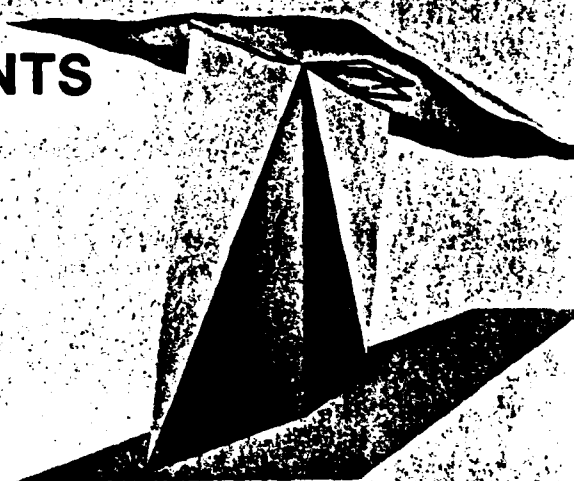
Technical Report 1143
August 1986
Interim Report for period
August 1980—July 1986

DTIC
SELECTED
APR 14 1987
S D

AD-A179 094

A NEW VERSION OF MODESRCH USING INTERPOLATED VALUES OF THE MAGNETOIONIC REFLECTION COEFFICIENTS

C. H. Shellman



Naval Ocean Systems Center
San Diego, California 92152

Approved for public release; distribution is unlimited.

87 4 14 003

NAVAL OCEAN SYSTEMS CENTER

San Diego, California 92152-5000

F. M. PESTORIUS, CAPT, USN
Commander

R. M. HILLYER
Technical Director

ADMINISTRATIVE INFORMATION

The work reported herein was conducted for the Defense Nuclear Agency over the period August 1980 to July 1986 under Project Number S99QMXBB.

Released by
J. A. Ferguson, Head
Modeling Branch

Under authority of
J. H. Richter, Head
Atmospheric Sciences
Division



UNCLASSIFIED

SECURITY CLASSIFICATION OF THIS PAGE

REPORT DOCUMENTATION PAGE

1a REPORT SECURITY CLASSIFICATION			1b RESTRICTIVE MARKINGS		
2a SECURITY CLASSIFICATION AUTHORITY UNCLASSIFIED			3 DISTRIBUTION/AVAILABILITY OF REPORT Approved for public release; distribution is unlimited.		
2b DECLASSIFICATION/DOWNGRADING SCHEDULE			5 MONITORING ORGANIZATION REPORT NUMBER(S)		
4 PERFORMING ORGANIZATION REPORT NUMBER(S) NOSC TR 1143			7a NAME OF MONITORING ORGANIZATION		
6a NAME OF PERFORMING ORGANIZATION Naval Ocean Systems Center		6b OFFICE SYMBOL (if applicable)	7b ADDRESS (City, State and ZIP Code)		
6c ADDRESS (City, State and ZIP Code) San Diego, CA 92152-5000		9 PROCUREMENT INSTRUMENT IDENTIFICATION NUMBER			
8a NAME OF FUNDING SPONSORING ORGANIZATION Defense Nuclear Agency Radiation Directorate		8b OFFICE SYMBOL (if applicable)	10 SOURCE OF FUNDING NUMBERS		
8c ADDRESS (City, State and ZIP Code) Washington, DC 20305		PROGRAM ELEMENT NO 62715H			
		PROJECT NO 599QMXBB			
		TASK NO 544-MP20			
		AGENCY ACCESSION NO DN651524			
11 TITLE (include Security Classification) A NEW VERSION OF MODESRCH USING INTERPOLATED VALUES OF THE MAGNETOIONIC REFLECTION COEFFICIENTS					
12 PERSONAL AUTHOR(S) C.H. Shellman					
13a TYPE OF REPORT Research		13b TIME COVERED FROM Aug 1980 TO July 1986		14 DATE OF REPORT (Year, Month, Day) August 1986	
				15 PAGE COUNT 30	
16 SUPPLEMENTARY NOTATION					
17 COSATI CODES			18 SUBJECT TERMS (Continue on reverse if necessary and identify by block number)		
FIELD	GROUP	SUB-GROUP	Radio propagation		
			Waveguide modes		
			Low-frequency propagation		
19 ABSTRACT (Continue on reverse if necessary and identify by block number) <p>For low-frequency (LF) cases of nighttime propagation, an elevated antenna, or distances close to the transmitter, the propagation constants for a large number of modes must be found to adequately represent the fields in the earth-ionosphere waveguide. Most of the cost in using MODESRCH to obtain these mode constants has been in performing full-wave integrations to obtain the reflection matrix, R. Until recently it had been necessary to carry out several full-wave integrations each for R and its derivative with respect to the angle of incidence, θ, for each waveguide mode. As a result of this present effort it has become possible to obtain interpolated values of R which are more than adequate to describe the earth-ionosphere mode constants.</p> <p>The approach used is to transform the reflection matrix, R, obtained from a full-wave integration, into magnetoionic reflection coefficients, R^{oe}. Each coefficient represents the complex amplitude of the ordinary or extraordinary component of the reflected wave given an incident wave which is polarized as either ordinary or extraordinary. The equations defining the magnetoionic eigenvectors, which are required for this transformation, have been derived for the free-space limit, so that they are applicable to a height that is below most of the ionization.</p> <p>Experience in use of the algorithm has shown that for eigenangles not too near branch points, the complex logs of the elements of R^{oe} vary so nearly linearly that values of R derived from interpolated values of $\ln R^{oe}$ are more than adequate for use in determining mode constants. An example is given for illustration. (continued next page)</p>					
20 DISTRIBUTION/AVAILABILITY OF ABSTRACT <input type="checkbox"/> UNCLASSIFIED/UNLIMITED <input checked="" type="checkbox"/> SAME AS RPT <input type="checkbox"/> DTIC USERS			21 ABSTRACT SECURITY CLASSIFICATION UNCLASSIFIED		
22a NAME OF RESPONSIBLE INDIVIDUAL C.H. Shellman			22b TELEPHONE (include Area Code) (619)225-2975		22c OFFICE SYMBOL Code 544

DD FORM 1473, 84 JAN

83 APR EDITION MAY BE USED UNTIL EXHAUSTED
ALL OTHER EDITIONS ARE OBSOLETE

UNCLASSIFIED

SECURITY CLASSIFICATION OF THIS PAGE

SECURITY CLASSIFICATION OF THIS PAGE (When Data Entered)

(19. continued)

It is believed that the reason for the nearly linear variation of the elements of R^{oe} is that each represents reflection from only one discrete complex height. Hence there is not the interference between waves reflected from different heights that would lead to the higher order variation of coefficients with change in incidence angle as seems to occur with elements of R . The approach used in this present effort in finding mode constants for low-frequency cases requiring a large number of modes results in considerable cost savings.

CONTENTS

I.	Introduction . . .	page 1
II.	Magnetoionic Components . . .	2
III.	Reflection Coefficients . . .	7
IV.	Branch Points . . .	8
V.	Interpolation . . .	10
VI.	Eigenangle Search using Triangular Mesh Units . . .	12
VII.	Example . . .	13
VIII.	Summary . . .	19
	References . . .	20

ILLUSTRATIONS

Figure

1. Search area . . . page 1
- 2(a). Branch cut for $z_d > h$. . . 3
- 2(b). Branch cut for $z_d < h$. . . 3
3. Search rectangle and associated triangular mesh pattern shown with hypothetical lines of $\text{Re}(F) = 0$ and $\text{Im}(F) = 0$ and eigenangles . . . 12



Accession For	
NTIS CRA&I	<input checked="" type="checkbox"/>
DTIC TAB	<input type="checkbox"/>
Unannounced	<input type="checkbox"/>
Justification	
By	
Distribution/	
Availability Codes	
Dist	Avail and/or Special
A-1	

TABLES

Table

1. Reflection coefficients . . . page 13
2. Complex logs of magnetoionic reflection coefficients . . . 14
3. Magnitude and phase of magnetoionic reflection coefficients and apparent complex heights of reflection . . . 15
4. Propagation parameters using full-wave solution values of R for each eigenangle . . . 17
5. Propagation paramaters using interpolated values of magnetoionic reflection coefficients . . . 18

I. INTRODUCTION

For low-frequency (LF) cases of nighttime propagation, an elevated antenna, or distances close to the transmitter, the propagation constants for a large number of modes must be found to adequately represent the fields in the earth-ionosphere waveguide. Most of the cost in using MODESRCH (Morfitt and Shellman, 1976) to obtain these mode constants has been in performing full-wave integrations to obtain the reflection matrix, \tilde{R} . Until recently it was necessary to carry out several full-wave integrations for \tilde{R} and its derivative with respect to the angle of incidence, θ , for each waveguide mode.

A means of using interpolated values of \tilde{R} is obtained in MODESRCH. The full-wave solutions are found at the four corners of each of a number of rectangles, and approximate values of elements of \tilde{R} are found using a third-order interpolation. The functional forms of the elements of \tilde{R} are sufficiently complicated, however, that they cannot be adequately approximated by the interpolation except for use in finding preliminary values used internally in MODESRCH.

It was perceived that some of the nonlinear variation of elements of \tilde{R} , especially in the LF range, might be due to interference of waves reflected from two fairly distinct complex altitudes. The relative phases of reflections from the two altitudes depend strongly on the angle of incidence, θ . The approach taken in the formulation described in sections II and III is to separate the reflection coefficients into ordinary and extraordinary components at a height that is below most of the ionization. Since neither component is expected to vanish, the complex logs of the elements of the magnetoionic reflection matrix may be used in the interpolation.

At each branch point there is an ambiguity in separating the ordinary and extraordinary components. A formulation for locating these points in the θ -plane is described in section IV. Near a branch point the elements of \tilde{R} are used as in MODESRCH.

There is an ambiguity in the relative number of whole cycles in the complex logs of the magnetoionic reflection coefficients at the four corners of the search rectangle, (figure 1).

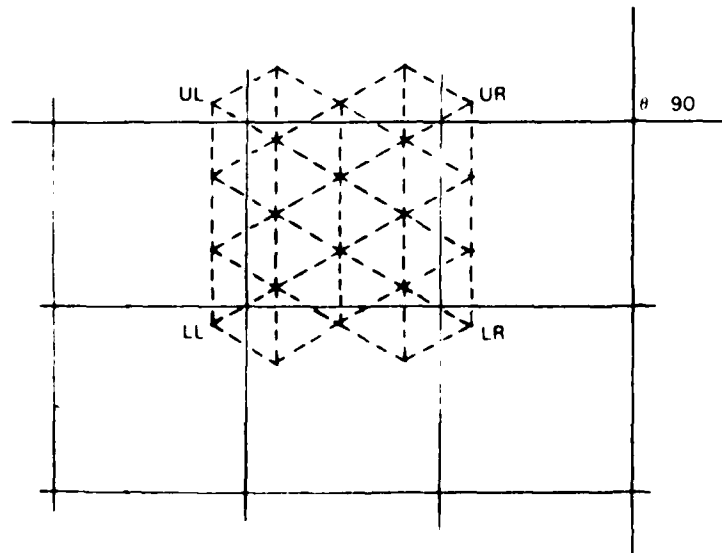


Figure 1. Search area.

This is resolved by choosing the numbers of cycles so as to minimize the magnitudes of the second- and third-order coefficients of the interpolation series. The formulation for obtaining the coefficients and for making the test is described in section V.

An example of use of the formulation presented in this report is given in section VII. The frequency used is 60 kHz, and a nighttime ionosphere model is used.

II. MAGNETOIONIC COMPONENTS

Decomposition of the reflection coefficients into ordinary and extraordinary components requires the magnetoionic eigenvectors at a height, z_d , that is below most of the ionization, that is, in the limit of small values of electron density. Since an earth curvature term is included in the full-wave solution for \underline{R} , this term is also included in the form for the eigenvectors.

The differential equation for the propagation of radio waves in the ionosphere, in the vertical direction, is given by Budden (1961) as

$$\vec{e}' = -i\kappa \underline{T} \vec{e} \quad , \quad (1)$$

where the elements of \vec{e} are E_x , $-E_y$, \mathcal{H}_x , \mathcal{H}_y . The matrix, \underline{T} , is defined by Budden (1961) and

$$i = (-1)^{1/2}$$

$$\kappa = \text{wave number.}$$

The prime denotes differentiation with respect to height, z .

Equation (1) may also be written as

$$\vec{w}' = -i\kappa \underline{T} \vec{w} \quad ,$$

where the elements of \vec{w} are labeled, in order, \mathcal{H}_y^u , E_y^u , \mathcal{H}_y^d and E_y^d . Also,

$$\underline{T} = \underline{L}^{-1} \underline{T} \underline{L} \quad ,$$

where

$$\underline{L} = \begin{pmatrix} q/p^2 & 0 & -q/p^2 & 0 \\ 0 & -1 & 0 & -1 \\ 0 & -q & 0 & q \\ 1 & 0 & 1 & 0 \end{pmatrix}$$

and

$$q = (C^2 + e)^{1/2} \quad \text{Re}(q) > 0$$

$$C = \cos \theta$$

$$e = 2(z_d - h)/r_e$$

$$p^2 = 1 + e$$

h = reference height for earth curvature

r_e = radius of the earth

z_d = height at which magnetoionic components are evaluated

The matrix, $\underline{\bar{L}}$, is defined in a way analogous to that of Budden (1961) but such that the superscripts u and d refer to upgoing and downgoing waves, respectively, at the height $z = z_d$, where, in general, $e \neq 0$. The branch cut for q is shown in figure 2.

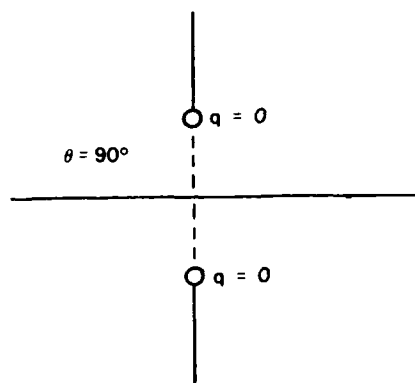


Figure 2a. Branch cut for $z_d > h$.

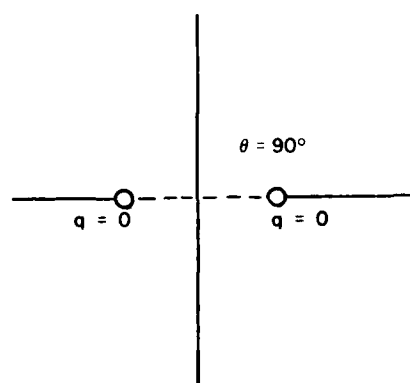


Figure 2b. Branch cut for $z_d < h$.

At this height and with a vanishingly small value of electron density, the matrix $\underline{\bar{T}}$ approaches being a diagonal matrix with elements q , q , $-q$, and $-q$. Hence, the characteristic upgoing waves at $z = z_d$ are uncoupled from the characteristic downgoing waves. However, since for either upgoing or downgoing waves the two eigenvalues of $\underline{\bar{T}}$ are the same (equal to q for upgoing waves and to $-q$ for downgoing waves), it is necessary to consider the terms of $\underline{\bar{T}}$ which are present for a very small, but otherwise negligible, value of electron density in order to determine the polarization of characteristic waves at the bottom of the ionosphere model. For this purpose only the upper left 2×2 submatrix of $\underline{\bar{T}}$ and the lower right 2×2 submatrix of $\underline{\bar{T}}$ are needed. These are used in the pair of matrix equations

$$\vec{w}'_{ud} = -i\kappa \underline{\bar{T}}_{ud} \vec{w}_{ud} ,$$

where

$$\vec{w}_{ud} = \begin{pmatrix} \mathcal{H}_y \\ E_y \end{pmatrix}_{ud} .$$

where the subscript ud refers to there being two sets of variables, one for upgoing waves and one for downgoing waves.

To form the matrices $\underline{\mathbb{I}}_{ud}$, the susceptibility matrix for very small values of electron density is needed. This may be written

$$\underline{\mathbb{M}} = C_M \begin{pmatrix} -\ell^2 G - 1/G & -n - \ell m G & m - \ell n G \\ n - \ell m G & -m^2 G - 1/G & -\ell - m n G \\ -m - \ell n G & \ell - m n G & -n^2 G - 1/G \end{pmatrix}.$$

where

$$C_M = iX/[U^2 Y(U^2 - Y^2)]$$

$$G = Y/(Z + i)$$

$$X = \text{normalized electron density}$$

$$Y = \text{normalized magnetic field strength}$$

$$Z = \nu/\omega$$

$$\nu = \text{collision frequency}$$

$$\omega = \text{angular wave frequency}$$

$$U = 1 - iZ$$

$$\ell = \sin \delta \cos \alpha$$

$$m = \sin \delta \sin \alpha$$

$$n = -\cos \delta$$

$$\delta = \text{codip angle}$$

$$\alpha = \text{azimuth of propagation measured east of north}$$

Note that the value of ν must correspond to the height, z_d , which is below most of the ionization. For MODE SRCH, the reference height, h , for earth curvature has usually been taken to be 50 km, but it may be set to the height of the base of the ionosphere or to some other height. Then

$$\underline{\mathbb{I}} = C_M \begin{pmatrix} S(m + n\ell G)/p^2 & S(\ell - mnG)/p^2 & 0 & \Gamma_{14} \\ 0 & 0 & 1 & 0 \\ -(n - \ell m G) & Q - m^2 G - 1/G & 0 & -S(\ell + mnG)/p^2 \\ P - \ell^2 G - 1/G & n + \ell m G & 0 & -S(m - n\ell G)/p^2 \end{pmatrix},$$

where

$$\Gamma_{14} = (Q - n^2 G - 1/G)/p^2 + q^2(n^2 G + 1/G)/p^4$$

$$S = \sin \theta$$

$$P = p^2/C_M$$

$$Q = q^2/C_M.$$

Finally,

$$\bar{\mathbf{T}} = C_T \begin{pmatrix} \Gamma - B^2 G & -(A + mBG)p^2 \\ A - mBG & \Gamma - m^2 p^2 G \end{pmatrix},$$

where

$$C_T = \pm_{ud} C_M / (2qp^2)$$

$$A = \ell S \pm_{ud} nq$$

$$B = -nS \pm_{ud} \ell q$$

$$\Gamma = p^2(2Q - 1/G)$$

$$\begin{aligned} \pm_{ud} &= + \text{ for upgoing waves} \\ &= - \text{ for downgoing waves} \end{aligned}$$

The condition for determining eigenvalues and vectors is then

$$\begin{pmatrix} -B^2 G - \lambda & -(A + mBG)p^2 \\ A - mBG & -m^2 p^2 G - \lambda \end{pmatrix} \begin{pmatrix} \mathcal{H}_y \\ E_y \end{pmatrix} = \begin{pmatrix} 0 \\ 0 \end{pmatrix}. \quad (2)$$

The eigenvalues are found from a solution of the characteristic equation

$$\lambda^2 + (B^2 + m^2 p^2)G\lambda + A^2 p^2 = 0.$$

Using the first row of the matrix in (2), the eigenvectors at the base of the ionosphere for either upgoing or downgoing waves are then given by

$$\mathbf{E}_{ud}^{(1)} = \begin{pmatrix} \mathcal{H}_{y1} & \mathcal{H}_{y1} \\ W + \xi & W - \xi \end{pmatrix},$$

where

$$\mathcal{H}_{y1} = 2(A + mBG)p^2$$

$$E_{y1} = W \pm_{oc} \xi$$

and where

$$W = (m^2 p^2 - B^2)G$$

$$\xi = [(B^2 + m^2 p^2)^2 G^2 - 4A^2 p^2]^{1/2} \quad (3)$$

It is the choice of the sign \pm_{oe} associated with ξ that distinguishes the "ordinary" waves from the "extraordinary" waves.

Using the second row of the matrix in (2), the matrix of eigenvectors may also be written

$$\underline{E}_{ud}^{(2)} = \begin{pmatrix} W - \xi & W + \xi \\ E_{y2} & E_{y2} \end{pmatrix}.$$

where

$$\mathcal{H}_{y2} = W \mp_{oe} \xi$$

$$E_{y2} = 2(A - mBG)$$

Neither $\underline{E}_{ud}^{(1)}$ nor $\underline{E}_{ud}^{(2)}$ is in normalized form. However, it can be seen that the two column vectors are given in the same order in the two matrices by noting that

$$\xi^2 = W^2 - \mathcal{H}_{y1} E_{y2}.$$

The form that is most manageable is derived by using the left column vector of $\underline{E}_{ud}^{(1)}$ and the right column vector of $\underline{E}_{ud}^{(2)}$ and normalizing the matrix so that the determinant is equal to unity. This results in

$$\underline{E}_{ud} = \begin{pmatrix} \mathcal{H}_{y1} & W + \xi \\ W + \xi & E_{y2} \end{pmatrix} [-2\xi(W + \xi)]^{-1/2},$$

where the sign of the square root, representing the value of ξ in (3), is chosen so that the sum $W + \xi$ has the larger magnitude in any one search rectangle. The eigenvector matrix, \underline{E}_{ud} , is singular for values of θ for which $\xi = 0$, that is, for which ordinary waves cannot be distinguished from extraordinary waves. Although not singular, it is not well conditioned for large collision frequency when the propagation is east-west at the equator.

Note that for a small value of G , that is, for a large value of collision frequency at the height z_d but not for east-west propagation at the equator, the matrix of eigenvectors is approximated by

$$\underline{E}_{ud} \text{ (large } \nu) \approx \begin{pmatrix} p & i \\ i & p^{-1} \end{pmatrix} / \sqrt{2} ,$$

representing nearly circularly polarized characteristic waves.

For east-west propagation at the equator, $\ell = n = 0$. In this case \underline{E}_{ud} becomes

$$\underline{E}_{ud} \text{ (equator east-west)} = \begin{pmatrix} 0 & i \\ i & 0 \end{pmatrix} .$$

The left eigenvector corresponds to ordinary waves since, for this case, $\mathcal{H}_y = 0$. For extraordinary waves $E_y = 0$ for east-west propagation at the equator (Budden, 1961).

III. REFLECTION COEFFICIENTS

Once the matrices of eigenvectors \underline{E}_u and \underline{E}_d are known, the elements of \underline{R}^{oe} may be found from those of \underline{R} and vice versa. The reflection matrix, \underline{R} , is as defined by Budden (1961). If the first columns of \underline{E}_u and \underline{E}_d correspond to ordinary waves, then \underline{R}^{oe} is of the form

$$\underline{R}^{oe} = \begin{pmatrix} R_{oo} & R_{oe} \\ R_{oe} & R_{ee} \end{pmatrix} .$$

where the first subscript refers to the polarization of the upgoing waves and the second subscript refers to that of the downgoing waves.

Matrices \underline{U}^{oe} and \underline{D}^{oe} are used to define upgoing and downgoing waves, respectively, where the elements of the first row of each represent values of \mathcal{H}_y and the elements of the second row of each represent values of E_y . The first columns of \underline{U}^{oe} and \underline{D}^{oe} correspond to the condition that, for the upgoing wave, $\mathcal{H}_y = 1$ and $E_y = 0$, and the second columns correspond to the condition that, for the upgoing waves, $\mathcal{H}_y = 0$ and $E_y = 1$. Then

$$\underline{U}^{oe} = \underline{E}_u^{-1}$$

$$\underline{D}^{oe} = \underline{E}_d^{-1} \underline{R}$$

and

$$\underline{R}^{oe} = \underline{D}^{oe} (\underline{U}^{oe})^{-1} = \underline{E}_d^{-1} \underline{R} \underline{E}_u .$$

The values are used in the interpolation scheme as "given" values at the upper corners of each search rectangle.

Approximate values of the elements of $\underline{\underline{R}}^{\text{oe}}$ found by interpolation must be transformed to values of elements of $\underline{\underline{R}}$. The first step is to form

$$\underline{\underline{U}} = \underline{\underline{E}}_u$$

$$\underline{\underline{D}} = \underline{\underline{E}}_d \underline{\underline{R}}^{\text{oe}}.$$

The elements of the first rows of $\underline{\underline{U}}$ and $\underline{\underline{D}}$ represent values of \mathcal{H}_y , and the elements of the second row of each represent values of E_y . The first columns of $\underline{\underline{U}}$ and $\underline{\underline{D}}$ correspond to the condition that the upgoing wave is ordinary, and the second columns of $\underline{\underline{U}}$ and $\underline{\underline{D}}$ correspond to the condition that the upgoing wave is extraordinary, if the first columns of $\underline{\underline{E}}_u$ and $\underline{\underline{E}}_d$ correspond to ordinary waves. Then

$$\underline{\underline{R}} = \underline{\underline{D}} \underline{\underline{U}}^{-1} = \underline{\underline{E}}_d \underline{\underline{R}}^{\text{oe}} \underline{\underline{E}}_u^{-1}.$$

Two effective complex heights of reflection may be found by considering that the diagonal elements, r_k , of $\underline{\underline{R}}^{\text{oe}}$ would be expected to vary as

$$dr_k/dC = 2i\kappa(h_k - z_d)r_k,$$

where $r_1 = R_{00}$, $r_2 = R_{ee}$, z_d is the height at which $\underline{\underline{R}}^{\text{oe}}$ is defined, and κ is the wave number. Then the effective heights of reflection are given by

$$h_k = z_d + \{d[\ln(r_k)]/dC\}/(2i\kappa)$$

It would be expected that the ordinary wave is reflected from the upper height (Budden, 1961) and that the reflection from this height is the stronger of the two.

IV. BRANCH POINTS

The reflection matrix $\underline{\underline{R}}$ cannot be resolved into ordinary and extraordinary components at points in the complex θ -plane where the argument of the square root, which is the expression for ξ , vanishes. Near these points the reflection matrix $\underline{\underline{R}}$ must be used in the search for the waveguide eigenangles without a transformation to the $\underline{\underline{R}}^{\text{oe}}$ form.

The expression (3) for ξ in section II may be written

$$\xi = (f_+ f_-)^{1/2},$$

where

$$f_{\pm} = (B^2 + m^2 p^2)G \pm 2Ap,$$

and where $\text{Re}(p) > 0$. There is a branch point at each value of θ for which either f_+ or f_- vanishes. This pair of conditions yields

$$f_{\pm} = [p^2 - (\kappa S_i + nq_i)^2] - G \pm 2p(\kappa S_i + nq_i) = 0, \quad (4)$$

for which a partial solution is

$$\begin{aligned} (\ell S_i + nq_i) &= t_i = p [1.0 \pm (1 + G^2)^{1/2}] / G & i = 1, 2 \\ &= -p [1.0 \pm (1 + G^2)^{1/2}] / G & i = 3, 4, \end{aligned}$$

where

$$S_i = (p^2 - q_i^2)^{1/2} \quad \text{Re}(S_i) > 0.$$

Note that the \pm_{ud} sign has been omitted so that values of q for both upgoing and downgoing waves are included in (4). The values of q at the branch points are then the solutions to

$$f_i = t_i - (\ell S_i - nq_i) = 0 \quad (5)$$

The solutions for $\ell = 0$ are $q_i = t_i/n$. For daytime ionosphere models, G is small at the base of the ionosphere model since $Z \gg Y$. In the limit of large collision frequency, $G \rightarrow 0$, and the two solutions are $q_i = 0, \infty$. For this case, then, there are branch points at $\theta = \cos^{-1}(\pm ie^{1/2})$. These are usually within about 10 deg of the 90-deg point in the θ -plane.

The solutions for a nonzero given value of ℓ , which is a function of the given values of codip and azimuth of propagation, are found by solving (5) for successively larger values of ℓ . Use is made of the derivatives

$$\begin{aligned} df_i/dq_i &= n - \ell q_i/S_i \\ d^2f_i/dq_i^2 &= -(\ell/S_i) (1 - q_i^2/S_i^2). \end{aligned}$$

For each new value of ℓ , the increment in q_i is

$$\begin{aligned} \Delta q_i &= -f_i / (df_i/dq_i) & df_i/dq_i \gg f_i (d^2f_i/dq_i^2) \\ &= -y_i \pm (y_i^2 - 2f_i)^{1/2} & \text{otherwise} \end{aligned}$$

where

$$y_i = (df_i/dq_i) / (d^2f_i/dq_i^2) \quad ,$$

and where the sign is chosen that yields the smallest magnitude of Δq_i .

The search is terminated when ℓ becomes equal to its originally specified value. Note that, with the condition $\text{Re}(S) > 0$, this yields four values of q_i . The branch points are then given by

$$\theta_i = \cos^{-1} C_i \quad ,$$

where

$$C_i = (q_i^2 - e)^{1/2}.$$

The sign of C_i is chosen so that the real part of C_i has the same sign as the real part of q_i . If the real part is positive, the branch point pertains to upgoing waves and to \underline{E}_u . Otherwise it pertains to downgoing waves and to \underline{E}_d .

V. INTERPOLATION

The interpolation, within each rectangle, is based on the reflection coefficients found from the full-wave solution at the corners of the rectangle. The four sets of reflection coefficients provide for interpolation in the third-order form

$$\underline{R} = \underline{R}_c + \underline{R}'_c (\theta - \theta_c) + \underline{R}''_c (\theta - \theta_c)^2/2 + \underline{R}'''_c (\theta - \theta_c)^3/6,$$

where θ_c is the value of θ at the center of the rectangle. The values of \underline{R}_c and its derivatives are considered to be in terms of coefficients such that

$$\underline{R}_c = a_0$$

$$\underline{R}'_c = a_1/t$$

$$\underline{R}''_c = 2a_2/t^2$$

$$\underline{R}'''_c = 6a_3/t^3,$$

where t is a real number representing the length in the θ plane from the center of the rectangle to any one of the corners.

For simplicity, the matrix notation is dropped at this point and the scalar variables are taken to refer to any one of the four elements of the reflection matrix. The elements of the coefficients are then given by

$$a_0 = [d_2^2 (R_{UL} + R_{LR}) - d_1^2 (R_{UR} + R_{LL})] / D_2$$

$$a_1 = [d_2^3 (R_{UL} - R_{LR}) - d_1^3 (R_{UR} - R_{LL})] / D_1$$

$$a_2 = [-(R_{UL} + R_{LR}) + (R_{UR} + R_{LL})] / D_2$$

$$a_3 = [-d_2 (R_{UL} - R_{LR}) + d_1 (R_{UR} - R_{LL})] / D_1,$$

where

$$d_1 = (\theta_{UL} - \theta_c)/t = -(\theta_{LR} - \theta_c)/t$$

$$d_2 = (\theta_{UR} - \theta_c)/t = -(\theta_{LL} - \theta_c)/t$$

$$D_1 = 2(d_2^2 - d_1^2)$$

$$D_2 = 2d_1d_2(d_2^2 - d_1^2).$$

The letter subscripts refer to the four corners of the rectangle (figure 1).

A measure of the adequacy of the interpolation series is needed so as to determine which rectangles need to be subdivided into smaller rectangles. For this purpose the two eigenvalues of the reflection matrix are used since it is inappropriate to require a close relative tolerance on weak elements of the matrix. They are given by

$$R_{\pm} = \{R_{11} + R_{22} \pm [(R_{11} - R_{22})^2 + 4R_{12}R_{21}]^{1/2}\}/2.$$

For purposes of determining the adequacy of the interpolation series, the values of the R_{\pm} found from the elements of the reflection matrix obtained from the full-wave solution are compared to the values of R_{\pm} found from elements of a best-fit second-order interpolation series. For this series a_3 is set to 0, and a_1 is found from

$$(a_1)_{LS} = [d_1^*(R_{UL} - R_{LR}) + d_2^*(R_{UR} - R_{LL})]/[2(d_1^*d_1 + d_2^*d_2)].$$

The measure of adequacy is then taken to be inverse to the largest of the eight values

$$e_+ = |(R_+)_{LS} - (R_+)_{FW}| / |(R_+)_{LS} + (R_+)_{FW}|$$

$$e_- = |(R_-)_{LS} - (R_-)_{FW}| / |(R_+)_{LS} + (R_+)_{FW}|$$

at the four corners of the rectangle.

The same formulation for interpolation is used for the complex logs of the magneto-ionic reflection coefficients. In the above equation R is then replaced by $\ln(R^{oe})$. However, for the case of complex logs of reflection elements there is an ambiguity in cycles of phase to be resolved. For this purpose it is noted that this phase ambiguity implies an ambiguity in the value of the coefficient a_3 such that its value might be different by

$$\Delta a_3 = (d_1n_1 - d_2n_2)2\pi/D_1,$$

where n_1 and n_2 are integers. Those values of n_1 and n_2 are chosen for which $|a_3 + \Delta a_3|$ is the smallest. Then $\ln(R_{UR}^{oe})$ and $\ln(R_{UL}^{oe})$ are modified by

$$\ln(R_{UR}^{oe}) \leftarrow \ln(R_{UR}^{oe}) + n_1 2\pi i$$

$$\ln(R_{UL}^{oe}) \leftarrow \ln(R_{UL}^{oe}) + n_2 2\pi i.$$

There is also an ambiguity in a_2 such that the value of a_2 might be different by

$$\Delta a_2 = 4n\pi/D_2,$$

where n is an integer. That value of n is chosen for which $|a_2 + \Delta a_2|$ is smallest. Then $\ln(R_{UR}^{oe})$ and $\ln(R_{LL}^{oe})$ are modified by

$$\ell n(R_{UR}^{oe}) \leftarrow \ell n(R_{UR}^{oe}) + 2n\pi i$$

$$\ell n(R_{LL}^{oe}) \leftarrow \ell n(R_{LL}^{oe}) + 2n\pi i$$

VI. EIGENANGLE SEARCH USING TRIANGULAR MESH UNITS

The search scheme formerly used in MODESRCH has been replaced with an algorithm using a mesh of equilateral triangles. A mesh of squares was used in the earlier algorithm. The basic principles are the same in the two versions. The mesh of equilateral triangles is used because it leads to simpler coding and because the function need only be evaluated at three corners of each mesh unit considered rather than at four.

As with the earlier version, each of one or more lines of constant phase is followed from one point on the perimeter of the search area to its point of exit, provided that any such line passes through the search area. The lines are defined by the condition that $\text{Im}(F) = 0$.

The chosen rectangular search area is shown in figure 3 along with the triangular mesh and hypothetical lines of $\text{Im}(F) = 0$. The search begins at the upper left corner of the mesh pattern and proceeds counterclockwise around the perimeter of the pattern. A phase line of $\text{Im}(F) = 0$ is detected by a change in sign of the $\text{Im}(F)$. Note that on one side of the

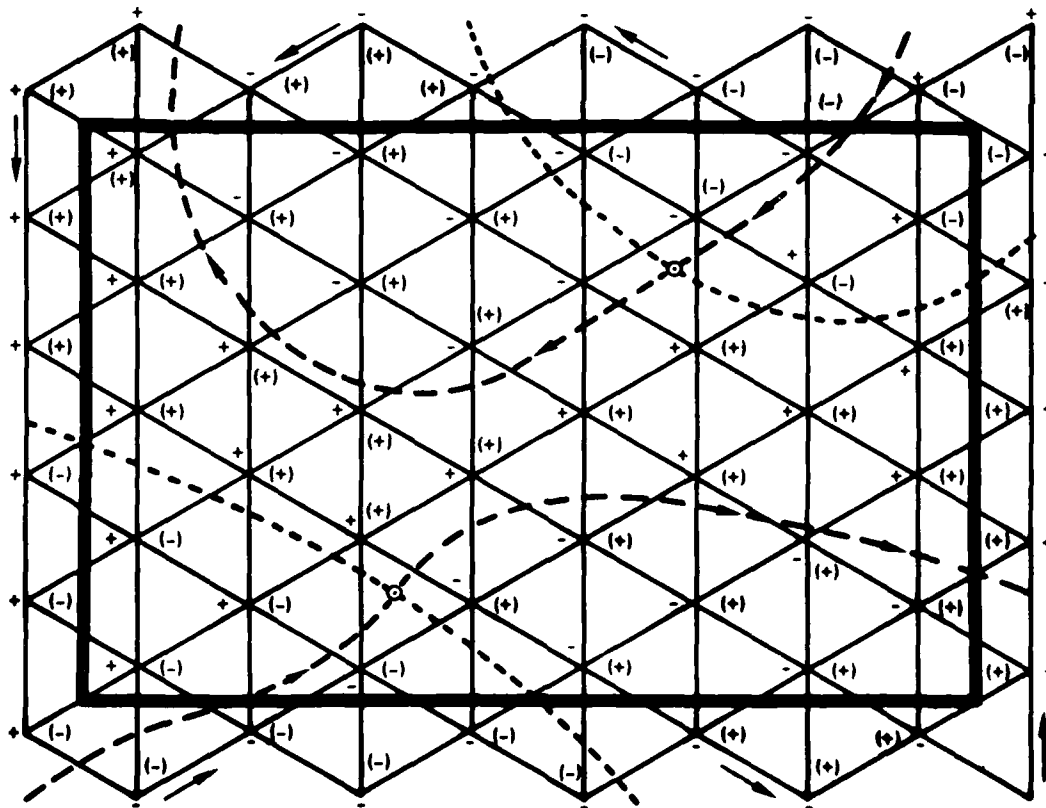


Figure 3. Search rectangle and associated triangular mesh pattern shown with hypothetical lines of $\text{Re}(F) = 0$ and $\text{Im}(F) = 0$ and eigenangles.

phase line $\text{Im}(F) > 0$ and on the other side $\text{Im}(F) < 0$. Each triangle along the line is checked for a line of $\text{Re}(F) = 0$ also passing through the triangle. Such a crossing of phase lines indicates the presence of a zero of the function F , hence a waveguide eigenangle. A Newton iteration is then used to locate the eigenangle in or near that triangle.

VII. EXAMPLE

The example given is that of a nighttime ionosphere model at a frequency of 60 kHz. In terms of parameters used in MODESRCH the electron density is specified as $\beta = 0.5$, $h' = 87$. The codip angle is 30 deg, and the geomagnetic azimuth of propagation is 35 deg east of north. The full-wave integration was carried out over a height range of 97 to 77 km altitude.

The elements of $(R + 1)/C$ are listed in table 1. These are the variables that were used in the previous version of MODESRCH for all search rectangles in the interpolation required for approximate starting values of eigenangles. They are used in the present version only for

Table 1. Reflection coefficients.

θ	$(11R_{11} + 1)/C$	$11R_{11}/C$	$1R_{11}/C$	$(1R_1 + 1)/C$
88	11.887+i9.143	-2.274+i9.323	-.634+i7.358	13.380-i15.865
86	11.280+i5.771	1.046+i5.148	1.498+i3.861	6.028-i7.086
84	9.948+i3.115	2.505+i2.021	2.353+i1.237	2.216-i0.907
82	8.488+i1.367	1.981-i0.525	1.631-i0.847	3.318+i3.994
80	7.197+i0.111	.036-i1.258	-.277-i1.266	7.848+i3.892
78	5.684-i0.900	-.805+i0.065	-.910+i0.150	8.267-i1.395
76	3.958-i1.058	.172+i0.684	.168+i0.759	3.385-i3.183
74	2.859-i0.383	.717-i0.141	.764-i0.125	.754+i0.037
72	2.703+i0.305	-.038-i0.768	-0.32-i0.817	2.858+i2.483
70	2.921+i0.355	-.771+i0.082	-.839-i0.072	5.094+i0.467
68	2.790+i0.065	-.200+i0.697	-.179+i0.802	3.182-i1.952
66	2.452+i0.007	.573+i0.292	.729+i0.284	.714-i0.653
64	2.317+i0.096	.336-i0.447	.373-i0.652	1.491+i1.521
62	2.302-i0.014	-.345-i0.336	-.579-i0.438	3.454+i0.856
60	2.049-i0.222	-.315+i0.265	-.490+i0.503	2.903-i1.150
58	1.665-i0.139	.200+i0.292	.415+i0.545	.940-i0.978
56	1.569+i0.167	.275-i0.150	.608-i0.312	.747+i0.707
54	1.782+i0.263	-.111-i0.265	-.188-i0.668	2.169+i1.053
52	1.890+i0.009	-.262+i0.072	-.705+i0.032	2.649-i0.247
50	1.647-i0.238	.023+i0.259	-.156+i0.699	1.530-i0.969

some selected rectangles and for very low ionosphere models. In table 2 are listed the values of the natural logs of the elements of the magnetoionic reflection coefficients. These variables are used for the interpolation used in the newer version of MODESRCH for most search rectangles.

Table 3 shows the magnitudes and phase values of the magnetoionic reflection matrices at "given" points on the real θ -axis. These points are at 2-deg intervals from 50 to 88 deg. Note that $|eR_e|$ (upper left element) is much larger than $|eR_o|$ (lower left element) for all values of θ and that $|oR_o|$ (lower right element) is larger than $|oR_e|$ for the stronger modes. This indicates that reflection is principally from two distinct complex heights. These effective heights are also listed in table 3.

Propagation parameters from the previous version of MODESRCH for the highest 44 modes are listed in table 4. In table 5 are given the propagation parameters from the newer version of MODESRCH. The eigenangles agree to ± 0.001 deg. The agreement for attenuation, phase velocity, excitation factor, and polarization is also more than adequate.

Table 2. Complex logs of magnetoionic reflection coefficients.

θ	eR_e	eR_o	oR_e	oR_o
88	-.215+i30.182	-2.743+i27.490	-2.017+i17.119	-.554+i20.463
86	-.199+i29.487	-2.711+i26.831	-2.063+i16.672	-.656+i20.178
84	-.173+i28.525	-2.651+i25.860	-2.204+i16.050	-.806+i19.765
82	-.147+i27.399	-2.546+i24.694	-2.498+i15.333	-.992+i19.259
80	-.128+i26.156	-2.418+i23.421	-3.046+i14.624	-1.206+i18.677
78	-.114+i24.822	-2.303+i22.068	-3.966+i14.426	-1.436+i18.021
76	-.097+i23.425	-2.195+i20.637	-3.599+i14.726	-1.659+i17.288
74	-.075+i21.995	-2.061+i19.161	-3.103+i13.892	-1.845+i16.477
72	-.050+i20.549	-1.908+i17.689	-2.847+i12.816	-1.975+i15.611
70	-.027+i19.091	-1.766+i16.226	-2.709+i11.704	-2.063+i14.724
68	-.002+i17.626	-1.639+i14.754	-2.683+i10.642	-2.152+i13.841
66	.031+i16.161	-1.502+i13.270	-2.818+i9.658	-2.286+i12.957
64	.073+i14.713	-1.346+i11.804	-3.148+i8.818	-2.490+i12.067
62	.123+i13.295	-1.184+i10.376	-3.524+i8.327	-2.747+i11.162
60	.176+i11.921	-1.032+i8.989	-3.392+i7.971	-3.015+i10.235
58	.216+i10.607	-.905+i7.645	-2.968+i7.214	-3.195+i9.321
56	.203+i9.350	-.824+i6.332	-2.624+i6.315	-3.236+i8.447
54	.130+i8.110	-.783+i5.017	-2.456+i5.423	-3.187+i7.584
52	.027+i6.868	-.752+i3.697	-2.468+i4.519	-3.124+i6.677
50	-.086+i5.632	-.718+i2.383	-2.639+i3.568	-3.100+i5.690

Table 3. Magnitude and phase of magnetoionic reflection coefficients and apparent complex heights of reflection.

$\theta = 88^\circ$	$\begin{pmatrix} .807 & .133 \\ .064 & .575 \end{pmatrix}$	$\begin{pmatrix} -70.7^\circ & -99.2^\circ \\ 135.1^\circ & 92.4^\circ \end{pmatrix}$	$82.80+i0.11$ $79.32-i0.83$
$\theta = 86^\circ$	$\begin{pmatrix} .820 & .127 \\ .066 & .519 \end{pmatrix}$	$\begin{pmatrix} -110.5^\circ & -124.8^\circ \\ 97.3^\circ & 76.1^\circ \end{pmatrix}$	$88.74+i0.25$ $81.07-i1.47$
$\theta = 84^\circ$	$\begin{pmatrix} .841 & .110 \\ .071 & .447 \end{pmatrix}$	$\begin{pmatrix} -165.7^\circ & -160.4^\circ \\ 41.6^\circ & 52.5^\circ \end{pmatrix}$	$89.08+i0.31$ $82.31-i1.94$
$\theta = 82^\circ$	$\begin{pmatrix} .863 & .082 \\ .078 & .371 \end{pmatrix}$	$\begin{pmatrix} 129.9^\circ & 158.5^\circ \\ -25.2^\circ & 23.5^\circ \end{pmatrix}$	$90.68+i0.26$ $83.27-i2.32$
$\theta = 80^\circ$	$\begin{pmatrix} .880 & .048 \\ .089 & .299 \end{pmatrix}$	$\begin{pmatrix} 58.6^\circ & 117.9^\circ \\ -98.1^\circ & -9.9^\circ \end{pmatrix}$	$91.96+i0.18$ $84.16-i2.60$
$\theta = 78^\circ$	$\begin{pmatrix} .893 & .019 \\ .100 & .238 \end{pmatrix}$	$\begin{pmatrix} -17.8^\circ & 106.5^\circ \\ -175.6^\circ & -47.5^\circ \end{pmatrix}$	$92.96+i0.17$ $85.08-i2.69$
$\theta = 76^\circ$	$\begin{pmatrix} .908 & .027 \\ .111 & .190 \end{pmatrix}$	$\begin{pmatrix} -97.8^\circ & 123.7^\circ \\ 102.4^\circ & -89.5^\circ \end{pmatrix}$	$93.64+i0.23$ $86.09-i2.46$
$\theta = 74^\circ$	$\begin{pmatrix} .928 & .045 \\ .127 & .158 \end{pmatrix}$	$\begin{pmatrix} -179.8^\circ & 76.0^\circ \\ 17.8^\circ & -135.9^\circ \end{pmatrix}$	$94.06+i0.28$ $87.00-i1.88$
$\theta = 72^\circ$	$\begin{pmatrix} .951 & .058 \\ .148 & .139 \end{pmatrix}$	$\begin{pmatrix} 97.3^\circ & 14.3^\circ \\ -66.5^\circ & 174.4^\circ \end{pmatrix}$	$94.39+i0.29$ $87.56-i1.24$
$\theta = 70^\circ$	$\begin{pmatrix} .973 & .067 \\ .171 & .127 \end{pmatrix}$	$\begin{pmatrix} 13.8^\circ & -49.4^\circ \\ -150.3^\circ & 123.6^\circ \end{pmatrix}$	$94.73+i0.28$ $87.76-i0.98$
$\theta = 68^\circ$	$\begin{pmatrix} .998 & .068 \\ .194 & .116 \end{pmatrix}$	$\begin{pmatrix} -70.1^\circ & -110.3^\circ \\ 125.3^\circ & 73.0^\circ \end{pmatrix}$	$95.03+i0.35$ $87.85-i1.30$
$\theta = 66^\circ$	$\begin{pmatrix} 1.031 & .060 \\ .223 & .102 \end{pmatrix}$	$\begin{pmatrix} -154.0^\circ & -166.6^\circ \\ 40.3^\circ & 22.4^\circ \end{pmatrix}$	$95.19+i0.47$ $88.03-i2.10$

Table 3. Continued.

$\theta = 64^\circ$	$\begin{pmatrix} 1.076 & .043 \\ .260 & .083 \end{pmatrix}$	$\begin{pmatrix} 123.0^\circ & 145.2^\circ \\ -43.7^\circ & -28.6^\circ \end{pmatrix}$	95.19+i0.59 88.39-i3.07
$\theta = 62^\circ$	$\begin{pmatrix} 1.131 & .029 \\ .306 & .064 \end{pmatrix}$	$\begin{pmatrix} 41.7^\circ & 117.1^\circ \\ -125.5^\circ & -80.5^\circ \end{pmatrix}$	95.04+i0.68 88.86-i3.59
$\theta = 60^\circ$	$\begin{pmatrix} 1.193 & .034 \\ .356 & .049 \end{pmatrix}$	$\begin{pmatrix} -37.0^\circ & 96.7^\circ \\ 155.0^\circ & -133.6^\circ \end{pmatrix}$	94.71+i0.67 89.23-i3.14
$\theta = 58^\circ$	$\begin{pmatrix} 1.241 & .051 \\ .405 & .041 \end{pmatrix}$	$\begin{pmatrix} -112.3^\circ & 53.3^\circ \\ 78.0^\circ & 174.1^\circ \end{pmatrix}$	94.19+i0.26 89.07-i1.48
$\theta = 56^\circ$	$\begin{pmatrix} 1.225 & .073 \\ .439 & .039 \end{pmatrix}$	$\begin{pmatrix} 175.7^\circ & 1.8^\circ \\ 2.8^\circ & 124.0^\circ \end{pmatrix}$	94.07-i0.65 88.77+i0.23
$\theta = 54^\circ$	$\begin{pmatrix} 1.139 & .086 \\ .457 & .041 \end{pmatrix}$	$\begin{pmatrix} 104.7^\circ & -49.3^\circ \\ -72.6^\circ & 74.6^\circ \end{pmatrix}$	94.48-i1.33 89.36+i0.96
$\theta = 52^\circ$	$\begin{pmatrix} 1.027 & .085 \\ .471 & .044 \end{pmatrix}$	$\begin{pmatrix} 33.5^\circ & -101.1^\circ \\ -148.2^\circ & 22.6^\circ \end{pmatrix}$	94.93-i1.61 90.61+i0.71
$\theta = 50^\circ$	$\begin{pmatrix} .918 & .071 \\ .488 & .045 \end{pmatrix}$	$\begin{pmatrix} -37.3^\circ & -155.6^\circ \\ 136.5^\circ & -34.0^\circ \end{pmatrix}$	95.28-i1.70 92.42+i0.01

Table 4. Propagation parameters using full-wave solution values of R for each eigenangle.

MODE	THETA	ATTEN	COVERC	WAIT MAG	WAIT ANG	THETAP	POL-MAG	POL-ANG
1	87 016	-0 120	1 195	0 99349	-92 151	0 342	0 26860	180 097
2	65 630	-0 255	3 728	0 99503	-47 007	0 560	2 92729	350 381
3	64 754	-0 055	0 990	0 99632	-50 300	0 255	0 27227	177 152
4	83 907	-0 170	3 465	0 99778	-11 728	0 375	3 38046	341 679
5	83 292	-0 044	0 989	0 99899	-21 967	-0 210	0 25243	134 516
6	82 799	-0 161	3 887	1 00003	1 590	0 097	3 32905	304 080
7	81 932	-0 058	1 557	1 00207	-19 263	-0 949	0 26454	71 548
8	81 496	-0 223	6 347	1 00317	1 489	0 059	3 24448	301 772
9	80 496	-0 061	1 943	1 00596	-25 093	-1 373	0 23828	51 344
10	79 980	-0 276	9 243	1 00751	0 362	0 050	4 39263	313 862
11	79 013	-0 062	2 286	1 01057	-30 251	4 360	0 20502	32 009
12	78 388	-0 325	12 581	1 01267	-0 351	0 035	5 65748	333 866
13	77 503	-0 065	2 684	1 01623	-32 583	3 643	0 18428	10 891
14	76 762	-0 370	16 291	1 01921	-0 836	0 017	5 84142	355 810
15	75 975	-0 065	3 162	1 02263	-31 505	3 002	0 18643	354 285
16	75 116	-0 409	20 211	1 02657	-1 181	-0 004	5 06413	10 445
17	74 433	-0 073	3 747	1 02993	-28 638	2 603	0 21306	345 491
18	73 453	-0 441	24 157	1 03496	-1 411	-0 029	4 18276	17 141
19	72 878	-0 079	4 487	1 03816	-25 377	2 403	0 26300	342 013
20	71 771	-0 466	27 996	1 04454	-1 493	-0 057	3 44938	18 518
21	71 311	-0 089	5 465	1 04738	-22 027	2 348	0 33234	340 765
22	70 066	-0 485	31 774	1 05534	-1 352	-0 082	2 87739	15 565
23	69 732	-0 102	6 766	1 05763	-18 658	2 436	0 41006	341 833
24	68 333	-0 504	35 789	1 06754	-0 947	-0 069	2 49803	7 986
25	68 145	-0 116	6 324	1 06897	-15 585	2 715	0 47931	347 574
26	66 573	-0 535	40 882	1 08124	-0 792	0 020	2 40732	356 860
27	66 550	-0 124	9 511	1 08147	-14 428	3 193	0 51133	358 132
28	64 933	-0 121	9 867	1 09531	-16 064	3 579	0 49946	7 400
29	64 797	-0 583	47 730	1 09647	-1 476	0 087	2 62925	347 981
30	63 285	-0 117	10 094	1 11070	-18 343	3 737	0 48140	11 680
31	63 012	-0 635	55 395	1 11333	-2 170	0 097	2 99662	344 031
32	61 613	-0 116	10 604	1 12776	-20 219	3 762	0 47019	12 324
33	61 212	-0 684	63 270	1 13199	-2 658	0 082	3 38499	343 633
34	59 912	-0 119	11 461	1 14555	-21 576	3 721	0 46496	11 594
35	59 387	-0 725	70 974	1 15273	-3 032	0 063	3 74394	345 389
36	58 183	-0 125	12 668	1 16759	-22 493	3 640	0 46914	10 873
37	57 528	-0 761	78 515	1 17591	-3 315	0 048	4 04386	348 786
38	56 422	-0 135	14 296	1 19086	-22 942	3 529	0 48884	10 267
39	55 628	-0 796	86 315	1 20192	-3 568	0 035	4 23061	353 596
40	54 627	-0 148	16 495	1 21677	-22 803	3 397	0 52681	9 453
41	53 655	-0 832	94 730	1 23118	-3 775	0 023	4 24517	359 020
42	52 743	-0 167	19 455	1 24570	-21 978	3 279	0 58183	8 774
43	51 693	-0 873	104 034	1 26422	-3 938	0 012	4 08341	3 790
44	50 916	-0 193	23 365	1 27613	-20 546	3 205	0 65289	9 080

Table 5. Propagation parameters using interpolated values of magnetoionic reflection coefficients.

MODE	THETA	ATTEN	VOVERC	WAIT MAG	WAIT ANG	THETAP	POL-MAG	POL-ANG
1	87 018	-0 120	1 195	-92 159	0 342	89 945	-6 508	180 100
2	85 630	-0 255	3 726	-47 004	0 559	89 803	-5 673	350 384
3	84 753	-0 056	0 991	-50 300	0 255	89 939	-4 859	177 149
4	83 907	-0 170	3 465	-11 727	0 375	89 723	-3 751	341 674
5	83 252	-0 044	0 969	-21 965	-0 210	89 879	-2 462	134 518
6	82 759	-0 161	3 887	-1 591	0 096	88 715	-0 909	304 069
7	81 932	-0 056	1 557	-19 263	-0 949	86 235	-0 124	71 549
8	81 496	-0 223	6 348	1 491	0 059	85 359	-0 412	301 744
9	80 476	-0 061	1 942	-25 105	-1 374	83 713	-0 093	51 338
10	79 979	-0 277	9 246	0 364	0 049	82 947	-0 395	313 534
11	79 013	-0 062	2 272	-30 346	4 371	81 629	-0 082	31 956
12	78 385	-0 325	12 585	-0 352	0 034	80 816	-0 414	333 624
13	77 503	-0 064	2 675	-32 716	3 613	79 717	-0 079	10 859
14	76 762	-0 371	16 308	-0 829	0 015	78 822	-0 441	357 534
15	75 976	-0 068	3 162	-31 510	3 002	77 899	-0 079	354 291
16	75 116	-0 409	20 207	-1 182	-0 004	76 905	-0 468	10 410
17	74 433	-0 073	3 745	-26 654	2 602	76 132	-0 082	345 497
18	73 493	-0 441	24 155	-1 411	-0 030	75 033	-0 491	4 18319
19	72 678	-0 079	4 466	-25 384	2 403	74 398	-0 087	0 26297
20	71 771	-0 466	27 996	-1 493	-0 057	73 183	-0 508	3 44904
21	71 311	-0 089	5 464	-22 039	2 349	72 684	-0 096	0 33227
22	70 066	-0 485	31 775	-1 359	-0 081	71 340	-0 521	2 87790
23	69 732	-0 102	6 766	-18 698	2 437	70 982	-0 109	0 41007
24	68 353	-0 505	35 794	-0 952	-0 069	69 490	-0 536	2 49841
25	68 145	-0 116	8 324	-15 586	2 715	69 291	-0 123	0 47931
26	66 573	-0 535	40 907	-0 808	0 019	67 629	-0 564	2 40810
27	66 550	-0 124	9 510	-14 429	3 193	67 605	-0 131	0 51135
28	64 933	-0 121	9 866	-16 064	3 579	65 909	-0 127	0 49942
29	64 797	-0 563	47 717	-1 464	0 088	65 766	-0 610	2 62913
30	63 287	-0 117	10 104	-18 319	3 738	64 191	-0 122	0 48159
31	63 012	-0 635	55 347	-2 155	0 095	63 905	-0 660	2 99058
32	61 613	-0 116	10 593	-20 240	3 759	62 453	-0 120	0 47007
33	61 212	-0 685	63 368	-2 655	0 081	62 038	-0 709	3 38906
34	59 912	-0 119	11 460	-21 578	3 721	60 695	-0 123	0 46495
35	59 365	-0 725	70 955	-3 026	0 063	60 151	-0 748	3 74649
36	58 183	-0 125	12 667	-22 500	3 639	58 913	-0 129	0 46912
37	57 528	-0 761	78 510	-3 323	0 048	58 238	-0 782	4 04522
38	56 423	-0 135	14 300	-22 948	3 529	57 104	-0 138	0 48880
39	55 629	-0 796	66 297	-3 572	0 034	56 289	-0 816	4 23251
40	54 627	-0 148	16 489	-22 807	3 397	55 263	-0 152	0 52672
41	53 551	-0 832	94 717	-3 779	0 022	54 298	-0 851	4 24591
42	52 793	-0 167	19 452	-21 973	3 279	53 387	-0 171	0 58179
43	51 693	-0 873	103 976	-3 929	0 013	52 263	-0 891	4 08353
44	50 918	-0 193	23 366	-20 541	3 204	51 473	-0 197	0 65304

VIII. SUMMARY

A formulation has been described that has made it possible to find LF earth-ionosphere waveguide mode constants at a much reduced cost and very low frequency (VLF) mode constants at less cost than previously. The most relevant cases are those for which a large number of modes are required, such as for short distances from the transmitter, nighttime propagation, or elevated antenna.

In contrast to the previous version of MODESRCH, the mode constants are functions of interpolated values of ionosphere reflection coefficients rather than of reflection coefficients found by a full-wave solution for the eigenangle associated with each mode. The given values for the interpolation are found with the full-wave solution only at selected points in the θ -plane. Examples indicate that the interpolated values are more than adequate for finding the values of the propagation mode constants.

A formulation is presented that appears to be effective in separating waves reflected from two rather distinct complex heights in the ionosphere. The advantage is that complications from the interference of the two waves tend to be avoided. Values of magnetoionic reflection coefficients found in the example indicate that adequate separation of components was accomplished for all values of the incidence angle, θ , required. The separation need not be complete for successful interpolation. It was more than adequate in the example, however, and especially complete for values of θ near 90 deg, where eigenangles sometimes are difficult to find using the previous version of MODESRCH.

The separation cannot be carried out in the vicinity of branch points, where magnetoionic eigenvectors cannot be clearly distinguished. In the example, no branch points occurred in the vicinity of the eigenangles. The formulation does allow for these branch points to be located, however, and their occurrence should present no problem since the procedure allows for defaulting to a method of solution more nearly like that used in the previous version of MODESRCH in the neighborhood of a branch point. Such cases are more likely to occur for cases of daytime ionosphere models than for nighttime.

The example is for a nighttime ionosphere at 60 kHz and for propagation over seawater. Forty-four eigenangles and associated mode constants were found in the interval of 50 to 90 deg in the real part of the incidence angle, θ . The cost was only about one-sixth that required for finding the same eigenangles and mode constants using the previous version of MODESRCH. Eigenangles differed at most by 0.001 deg.

REFERENCES

- Budden, K.G. (1955), The Numerical Solution of Differential Equations Governing Reflexion of Long Radio Waves From the Ionosphere, Proceedings, Royal Society (London), Vol A227, p 516-537.
- Budden, K.G. (1961), Radio Waves in the Ionosphere, Cambridge University Press.
- Morfitt, D.G., and C.H. Shellman (1976), "MODESRCH," an Improved Computer Program for Obtaining Elf/Vlf/Lf Mode Constants in an Earth-Ionosphere Waveguide, DNA Interim Report No. 77T.

DISTRIBUTION LIST

DEPARTMENT OF DEFENSE

DEPUTY UNDER SECRETARY OF DEFENSE
CMD, CONT, COMM & INTELL
DEPARTMENT OF DEFENSE
WASHINGTON, DC 20301

DIRECTOR
COMMAND CONTROL TECHNICAL CENTER
11440 ISAAC NEWTON SQUARE, N
RESTON, VA 22091
C-650

DIRECTOR
COMMAND CONTROL TECHNICAL CENTER
ROOM ME682, THE PENTAGON
WASHINGTON, DC 20301
C-312

DIRECTOR
DEFENSE ADVANCED RESEARCH PROJECT
AGENCY
1440 WILSON BLVD
ARLINGTON, VA 22209
NUCLEAR MONITORING RSCH
STRATEGIC TECH OFFICE

DEFENSE COMMUNICATION ENGINEERING CENTER
1860 WIEHLE AVENUE
RESTON, VA 22090
CODE R220 (M HOROWITZ)
CODE R410
CODE R103

DIRECTOR
DEFENSE COMMUNICATIONS AGENCY
WASHINGTON, DC 20305
CODE 810
CODE 480
CODE 101B

DEFENSE COMMUNICATIONS AGENCY
WWMCCS SYSTEM ENGINEERING ORG
WASHINGTON, DC 20305
RL CRAWFORD

DEFENSE TECHNICAL INFORMATION CENTER
CAMERON STATION
ALEXANDRIA, VA 22314

DIRECTOR
DEFENSE INTELLIGENCE AGENCY
WASHINGTON, DC 20301
DIAST 5
DB-4C (EDWARD O'FARRELL)

DIRECTOR
DEFENSE NUCLEAR AGENCY
WASHINGTON, DC 20305
DDST
TITL TECH LIBRARY
RAAE
STVL

DIRECTOR
JOINT STRAT TGT PLANNING STAFF JCS
OFFUTT AFB
OMAHA, NB 68113
JPST

COMMANDER
FIELD COMMAND
DEFENSE NUCLEAR AGENCY
KIRTLAND AFB, NM 87115
FCPR

DIRECTOR INTERSERVICE NUCLEAR WEAPONS SCHOOL
KIRTLAND AFB, NM 87115
DOCUMENT CONTROL

CHIEF
LIVERMORE DIVISION FLD COMMAND DNA
LAWRENCE LIVERMORE LABORATORY
PO BOX 808
LIVERMORE, CA 94550
FCPRL

DIRECTOR
NATIONAL SECURITY AGENCY
FT GEORGE G MEADE, MD 20755
W65
OLIVER H BARTLETT W32
TECHNICAL LIBRARY
JOHN SKILLMAN R52

OJCS/J-3
THE PENTAGON
WASHINGTON, DC 20301
OPERATIONS (WWMCCS EVAL
OFF, MR TOMA)

OJCS/J-5
THE PENTAGON
WASHINGTON, DC 20301
PLANS & POLICY (NUCLEAR DIVISION)

UNDER SECY OF DEFENSE FOR RESEARCH
AND ENGINEERING
DEPARTMENT OF DEFENSE
WASHINGTON, DC 20301
S&SS (OS)

DEPARTMENT OF THE ARMY
COMMANDER/DIRECTOR
ATMOSPHERIC SCIENCES LABORATORY
US ARMY ELECTRONICS COMMAND
WHITE SANDS MISSILE RANGE, NM 88002
DELAS-AE-M (FE NILES)

COMMANDER
HARRY DIAMOND LABORATORIES
2800 POWDER MILL RD
ADELPHI, MD 20783
DELHD-NP (FN WIMENITZ)
MILDRED H WEINER DRXDO-II

COMMANDER
US ARMY FOREIGN SCIENCE & TECH CENTER
220 7TH STREET, NE
CHALOTTESVILLE, VA 22901
R JONES
PA CROWLEY

COMMANDER
US ARMY NUCLEAR AGENCY
7500 BACKLICK ROAD
BUILDING 2073
SPRINGFIELD, VA 22150
MONA-WE (J BERBERE?)

CHIEF
US ARMY RESEARCH OFFICE
PO BOX 12211
TRIANGEL PARK, NC 27709
DRXRD-ZC

DEPARTMENT OF THE NAVY
CHIEF OF NAVAL OPERATIONS
NAVY DEPARTMENT
WASHINGTON, DC 20350
OP 941
OP-604C3
OP 943
OP 981

CHIEF OF NAVAL RESEARCH
NAVY DEPARTMENT
ARLINGTON, VA 22217
CODE 402
CODE 420
CODE 421
CODE 461
CODE 464

COMMANDING OFFICER
NAVAL INTELLIGENCE SUPPORT CENTER
4301 SUTLAND RD BLDG 5
WASHINGTON, DC 20390

OFFICER-IN-CHARGE
WHITE OAK LABORATORY
NAVAL SURFACE WEAPONS CENTER
SILVER SPRING, MD 20910
CODE WA501 NAVY NUC PRGMS OFF
CODE WX21 TECH LIBRARY

COMMANDER
NAVAL TELECOMMUNICATIONS COMMAND
NAVTELCOM HEADQUARTERS
4401 MASSACHUSETTS AVE, NW
WASHINGTON, DC 20390
CODE 24C

COMMANDING OFFICER
NAVY UNDERWATER SOUND LABORATORY
FORT TRUMBULL
NEW LONDON, CT 06320
PETER BANNISTER
DA MILLER

DIRECTOR
STRATEGIC SYSTEMS PROJECT OFFICE
NAVY DEPARTMENT
WASHINGTON, DC 20376
NSP-2141

DEPARTMENT OF THE AIR FORCE
COMMANDER
ADC/DC
ENT AFB, CO 80912
DC (MR LONG)

COMMANDER
ADCOM/XPD
ENT AFB, CO 80912
XPQDQ
XP

AF GEOPHYSICS LABORATORY, AFSC
HASCOM AFB, MA 01731
CRU (S HOROWITZ)

AF WEAPONS LABORATORY, AFSC
KIRTLAND AFB, NM 87117
SUL (2)
DYC

COMMANDER
ROME AIR DEVELOPMENT CENTER, AFSC
GRIFFISS AFB, NY 13440
EMTLD DOC LIBRARY

COMMANDER
ROME AIR DEVELOPMENT CENTER, AFSC
HANSOM AFB, MA 01731
EEP JOHN RASMUSSEN

COMMANDER IN CHIEF
STRATEGIC AIR COMMAND
OFFUTT AFB, NB 68113
NRT
XPFS

LAWRENCE LIVERMORE NATIONAL
LABORATORY
PO BOX 808
LIVERMORE, CA 94550
TECH INFO DEPT L-3

LOS ALAMOS NATIONAL SCIENTIFIC
LABORATORY
PO BOX 1663
LOS ALAMOS, NM 87545
DOC CON FOR T F TASCHEK
DOC CON FOR D R WESTERVELT
DOC CON FOR P W KEATON

SANDIA LABORATORY
LIVERMORE NATIONAL LABORATORY
PO BOX 969
LIVERMORE, CA 94550
DOC CON FOR B E MURPHEY
DOC CON FOR T B COOK ORG 8000

SANDIA NATIONAL LABORATORY
PO BOX 5800
ALBUQUERQUE, NM 87115
DOC CON FOR SPACE PROJ DIV
DOC CON FOR A D THORNBROUGH
DOC CON FOR 3141 SANDIA RPT COLL

OTHER GOVERNMENT
DEPARTMENT OF COMMERCE
NATIONAL BUREAU OF STANDARDS
WASHINGTON, DC 20234
RAYMOND T MOORE

DEPARTMENT OF COMMERCE
OFFICE OF TELECOMMUNICATIONS
INSTITUTE FOR TELECOM SCIENCE
BOULDER, CO 80302
WILLIAM F UTLAUT
L A BERRY
A GLENN JEAN

DEPARTMENT OF DEFENSE CONTRACTORS
AEROSPACE CORPORATION
PO BOX 92957
LOS ANGELES, CA 90009
IRVING M GARFUNKEL

ANALYTICAL SYSTEMS ENGINEERING CORP
5 OLD CONCORD RD
BURLINGTON, MA 01803
RADIO SCIENCES

THE BOEING COMPANY
PO BOX 3707
SEATTLE, WA 98124
GLENN A HALL
J F KENNEY

ESL, INC
495 JAVA DRIVE
SUNNYVALE, CA 94086
JAMES MARSHALL

GENERAL ELECTRIC COMPANY
SPACE DIVISION
VALLEY FORGE SPACE CENTER
GODDARD BLVD KING OF PRUSSIA
PO BOX 8555
PHILADELPHIA, PA 19101
SPACE SCIENCE LAB (MH BORTNER)

KAMAN TEMPO
816 STATE STREET
PO DRAWER QQ
SANTA BARBARA, CA 93102
B GAMBILL
DASIAC
WARREN S KNAPP

GTE SYLVANIA, INC
ELECTRONICS SYSTEMS GRP
EASTERN DIVISION
77 A STREET
NEEDHAM, MA 02194
MARSHAL CROSS

ITT RESEARCH INSTITUTE
10 WEST 35TH STREET
CHICAGO, IL 60616
TECHNICAL LIBRARY

UNIVERSITY OF ILLINOIS
DEPARTMENT OF ELECTRICAL ENGINEERING
URBANA, IL 61803
AERONOMY LABORATORY

JOHNS HOPKINS UNIVERSITY
APPLIED PHYSICS LABORATORY
JOHNS HOPKINS ROAD
LAUREL, MD 20810
J NEWLAND
PT KOMISKE

LOCKHEED MISSILE & SPACE CO, INC
3251 HANOVER STREET
PALO ALTO, CA 94304
E E GAINES
W L IMHOF D/52-12
J B REAGAN D652-12
R G JOHNSON D/52-12

MASSACHUSETTS INSTITUTE OF TECHNOLOGY
LINCOLN LABORATORY
PO BOX 73
LEXINGTON, MA 02173
D M TOWLE

MISSION RESEARCH CORPORATION
735 STATE STREET
SANTA BARBARA, CA 93101
R HENDRICK
F FAJEN

MITRE CORPORATION
PO BOX 209
BEDFORD, MA 01730
G HARDING

PACIFIC-SIERRA RESEARCH CORP
1456 CLOVERFIELD BLVD
SANTA MONICA, CA 90404
E C FIELD, JR

PENNSYLVANIA STATE UNIVERSITY
IONOSPHERIC RESEARCH LABORATORY
318 ELECTRICAL ENGINEERING EAST
UNIVERSITY PARK, PA 16802
IONOSPHERIC RSCH LAB

R&D ASSOCIATES
PO BOX 9695
MARINA DEL REY, CA 90291
FORREST GILMORE
WILLIAM J KARZAS
PHYLLIS GREIFINGER
CARL GREIFINGER
H A ORY
BRYAN GABBARD
R P TURCO
SAUL ALTSCHULER

RAND CORPORATION
1700 MAIN STREET
SANTA MONICA, CA 90406
TECHNICAL LIBRARY
CULLEN CRAIN

SRI INTERNATIONAL
333 RAVENSWOOD AVENUE
MENLO PARK, CA 94025
DONALD NEILSON
GEORGE CARPENTER
W G CHETNUT
J R PETERSON
GARY PRICE

STANFORD UNIVERSITY
RADIO SCIENCE LABORATORY
STANFORD, CA 94305
R A HELLIWELL
FRASER SMITH
J KATSUFRAKIS

CALIFORNIA INSTITUTE OF TECHNOLOGY
JET PROPULSION LABORATORY
4800 OAK GROVE DRIVE
PASADENA, CA 91103
ERNEST K SMITH